P2.2 Cross-mountain Airflow as Observed from Flight Data Recorder (FDR) Data of Transport Category Commercial Aircraft

P.W. Chan * and C.M. Shun
Hong Kong Observatory, Hong Kong, China

1. INTRODUCTION

The Hong Kong International Airport (HKIA) is situated in an area of complex terrain. To the south of it is the mountainous Lantau Island with peaks rising to about 1 km AMSL and valleys as low as several hundred metres in between. The complex terrain leads to airflow disturbances in the airport area, bringing windshear and turbulence to landing and departing aircraft at HKIA.

The Hong Kong Observatory (HKO) operates a suite of in-situ and remote-sensing instruments to monitor the airflow in the airport area. Among them, the Doppler LIght Detection and Ranging (LIDAR) systems installed in the middle of the airfield command a good view of the runway corridors and provide valuable information in the detection of low-level windshear and turbulence. To study the terrain-disrupted airflow in detail, HKO also obtains FDR/QAR (Quick Access Recorder) data of transport category commercial aircraft from the local airlines.

Using an algorithm and associated software developed by the National Aerospace Laboratory (NLR) of The Netherlands (Haverdings, 2000 and 2006), FDR data of selected aircraft fleets were analyzed to derive atmospheric quantities including the three components of the wind and the turbulent kinetic energy (TKE, as a measure of turbulence intensity). The wind data derived from the NLR software is believed to be more accurate than those available directly from the FDR/QAR data since aircraft aerodynamic factors (e.g. sideslip angle, angle-of-attack) are considered by the algorithm.

This paper summarizes the FDR data analysis results in two typical cases of terrain-disrupted airflow at HKIA, namely, east to southeasterly airstream in spring-time and gale-force southeasterly flow associated with a typhoon in the summer. The objective of the study is to see how these in-situ aircraft measurements provide additional insights about the nature of the wind disturbances.

2. SPRING-TIME CASE: 30 MARCH 2005

This is a typical east to southeasterly wind case in spring-time – the peak windshear and turbulence season at HKIA. The fresh to strong airflow crossing the mountains on Lantau Island together with a stable boundary layer favoured the occurrence of airflow disturbances over the airport area. At 23:27 UTC, 29 March 2005 (7:27 a.m., 30 March 2005, with HKT = UTC + 8 hours), a B744 aircraft landing at the south runway of HKIA from the west reported encountering of significant windshear (headwind gain of 40 knots) and moderate turbulence. FDR data were obtained from this flight after the event. The analysis of this case is described in detail in Haverdings (2006). The following is a summary of the major observations of the FDR analysis:

(a) When the aircraft was still sufficiently far away from Lantau Island (4 nautical miles from western end of the south runway), it encountered fresh to strong east-southeasterly winds (Figure 1). As the aircraft came closer to the airport, there was a significant drop of the horizontal wind speed, with a minimum of only a couple m/s momentarily at about 2.5 nautical miles from the runway. After that, the wind speed increased again and reached a maximum of 17 m/s at 1.3 nautical miles. The length scale of this wind change (2.5 – 1.3 = 1.2 nautical miles) is within the windshear scale (4 km). The magnitude of the change (~15 m/s) is close to the pilot report of windshear encounter, though it is still ~5 m/s smaller, probably due to effect of automatic/manual control of the airspeed (Haverdings 2006). It could be seen from Figure 1 that, within the region of wind speed change, the wind direction also fluctuated rapidly.

(b) The vertical wind velocity (Figure 2) exhibits "roller coaster" variation between upward motion of 4 m/s and downward motion of 6 m/s. The length scale of the change is in the order of 0.5 nautical mile.

(c) The TKE (Figure 2) also shows rapid fluctuations. The maximum TKE is about 10 m^2/s^2, which is larger than the level of "heavy turbulence" (7.2 m^2/s^2, Haverdings 2006).

The above observations are consistent with the LIDAR velocity data (Figure 3) which shows that there is a mountain wake of weaker but more turbulent flow between 1.5 and 3 nautical miles to the west of the south runway.

To analyze this case in more detail, numerical simulation of the airflow is performed using the Regional Atmospheric Modelling System (RAMS) version 4.4 in four nested grids as initialized at 18 UTC, 29 March 2005, with the same setting as in the large-eddy simulation performed in Chan (2006). The simulated wind component along the LIDAR's measurement radial at about the same time of this windshear event shows the presence of a mountain wake to the northwest of Lantau Island (Figure 4), though the wake is not so extensive. As such, a vertical cross section is made right inside the wake in the simulated result, instead of directly over the arrival corridor of the south runway, to show the vertical velocity distribution (Figure 5). The vertical velocity is found to also exhibit "roller coaster" behaviour with a length scale similar to the actual observations within the mountain wake region, but the magnitude is a bit

* *Corresponding author address:* P.W. Chan, Hong Kong Observatory, 134A Nathan Road, Hong Kong email: pwchan@hko.gov.hk

smaller (between +3 m/s and -2 m/s). Bands of upward and downward motion with northwest-to-southeast orientation are also found in this wake region (Figure 6). The TKE field from the simulation also has larger values in the mountain wake area (not shown). In summary, the flight data from the arriving aircraft are generally consistent with the LIDAR observations and numerical forecast.

3. TYPHOON CASE: 2-3 AUGUST 2006

In this case, we focus on the change of the wind pattern at the airport area when the background wind direction shifted as a tropical cyclone moved towards the south China coast relative to Hong Kong. In the evening of 2 August, Typhoon Prapiroon was located to the south of Hong Kong and brought gale force easterly winds to HKIA (Figure 7(a)). FDR data were obtained from five aircraft which landed at the north runway of HKIA from the west between 11 and 13 UTC, 2 August. The following features are observed from these data:

(a) The horizontal wind speed exhibits quite rapid fluctuations (Figure 7(b)), but they mostly change by within 5 m/s over a distance of 0.3 – 0.5 nautical mile.
(b) The wind direction mainly fluctuates between 60 and 100 degrees (Figure 7(c)). It occasionally backs to 20 – 40 degrees, but only lasts for a very short duration (0.25 second).
(c) The TKE gets to quite large values (Figure 7(d)), all reaching the level of "heavy turbulence" except one flight.

In the afternoon of the following day, Prapiroon moved to the southwest of Hong Kong and brought gale-force southeasterly winds to HKIA. The LIDAR velocity image showed that the airflow at HKIA was more disturbed with many small-scale features (in the order of several hundred metres) to the northwest of Lantau Island (Figure 7(e)). FDR data were obtained from three flights between 05 and 07 UTC, 3 August, and the followings are observed:

(a) The horizontal wind speed shows more rapid fluctuations (Figure 7(f)) compared with the evening of 2 August. The wind change could be up to 5 – 10 m/s over a distance of 0.5 nautical mile or so.
(b) Compared with 2 August, the wind direction veers and mostly varies between 80 and 120 degrees (Figure 7(g)). It sometimes backs to 40 degrees and, compared with 2 August, it stays there for a longer duration (about 1 second).
(c) The TKE is much larger than the previous evening (Figure 7(h)). It occasionally reaches 20 – 40 m^2/s^2, which was not attained in the evening of 2 August.

The above comparison between the FDR data at two different time slots shows that the properties of the wind disturbance over the airport area changed as the background wind direction shifted due to movement of the tropical cyclone relative to Hong Kong. In particular, when the wind over Hong Kong gained more southerly component and became stronger, the disruption by Lantau terrain became more significant and the airflow had greater turbulence. To further study the length scale of the wind fluctuations over the airport area, spectral analysis is performed with the horizontal wind speeds (in 4 Hz) from the FDR data. The results for the evening of 2 August and the afternoon of 3 August are shown in Tables 1(a) and 1(b) respectively. A typical power spectrum at each time slot is given in Figure 8. At around 12 UTC on 2 August, the major spectral peaks from the five flights in the study have spatial scale between 920 and 7400 m. At around 06 UTC on 3 August, the corresponding spatial scale from the three flights lies between 490 and 3700 m. It is apparent that the horizontal spatial scale of the horizontal wind speed fluctuations reduced by about half from the evening of 2 August to the afternoon of the next day. A similar analysis is conducted for the vertical velocity. The spectral analysis results are summarized in Table 2. For both time periods considered here, there does not appear to have a change in the horizontal spatial scale of the vertical velocity fluctuations. The difference in spatial scales of horizontal wind speed and vertical velocity fluctuations might indicate that the terrain-disrupted flow features (e.g. eddies, wind streaks, etc.) could have anisotropic structures (in the horizontal and vertical dimensions).

4. CONCLUSIONS

The FDR data in the two typical cases of terrain-disrupted airlfow in the vicinity of HKIA are studied in this paper, namely, east to southeasterly wind in the spring-time windshear peak season and gale-force winds associated with a typhoon in the summer. In the former case, the FDR data vividly reveals the mountain wake characteristics of Lantau Island. The horizontal wind speed could change by as large as ~15 m/s across the wake, and the wind direction shows rapid fluctuations. The vertical velocity exhibits "roller coaster" behaviour and the TKE reaches the level of "heavy turbulence" inside the wake. All these features are consistent with the LIDAR observations that the mountain wake has weaker horizontal speeds but more turbulent flow compared with the strong background east to southeasterly wind. These features are also observed in the numerical simulation results.

In the second case, the FDR data provide valuable insight into the change of the wind fluctuations over the airport area as the tropical cyclone moves relative to Hong Kong. As the wind veered from easterly to southeasterly over Hong Kong, the airflow became more turbulent over HKIA with more significant fluctuations of the horizontal wind speed (reaching 10 m/s over 0.5 nautical mile, viz. windshear), backing of the wind for longer duration (suggesting more persistent wavy motion) as well as larger value of TKE (to a level far exceeding the "heavy turbulence" threshold). The length scale of horizontal wind speed fluctuation also reduced by half as determined from spectral analysis.

Acknowledgement

The authors would like to thank Cathay Pacific Airways for providing the FDR data in this study.

References

Chan, P.W., 2006: Super-high-resolution numerical simulation of atmospheric turbulence in an area of complex terrain. *12th Conference on Mountain Meteorology*, American Meteorological Society, New Mexico, U.S.A.

Haverdings, H., 2000: Updated specification of the WINDGRAD algorithm. NLR TR-2000-63, National Aerospace Laboratory.

Haverdings, H., 2006: FDR analysis of 3 cases delivered by Hong Kong Observatory. NLR-CR-2006-114, National Aerospace Laboratory.

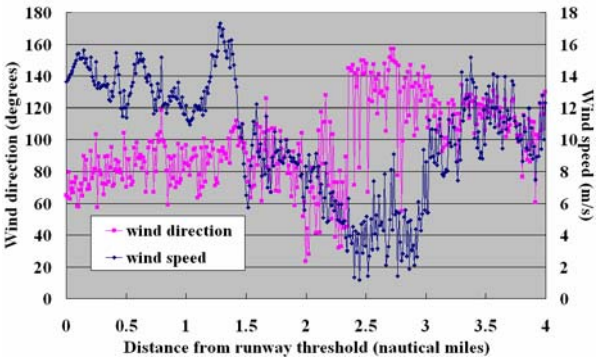

Figure 1 Wind speed and direction up to 4 nautical miles from the runway for the flight at 23:27 UTC, 29 March 2005.

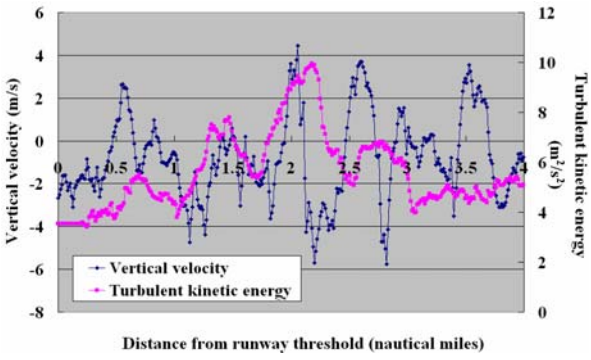

Figure 2 Vertical velocity and TKE up to 4 nautical miles from the runway for the flight at 23:27 UTC, 29 March 2005.

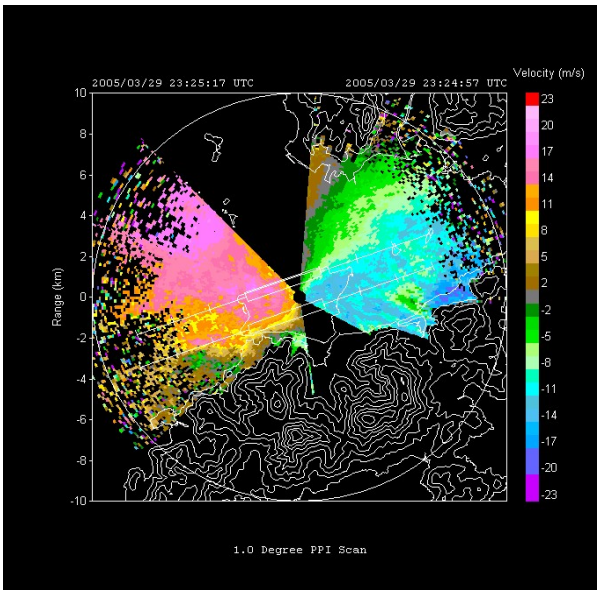

Figure 3 LIDAR's velocity image from 1-degree conical scan at 23:25 UTC, 29 March 2005. The tick marks on the extended runway centrelines indicate 1, 2 and 3 nautical miles from the runway ends.

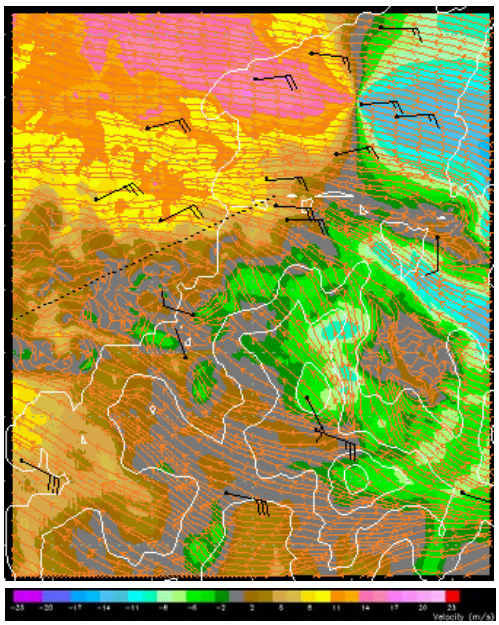

Figure 4 Model-simulated velocity component of the LIDAR's radial at 50 m AMSL (colour shading) and wind at the surface (wind barbs).

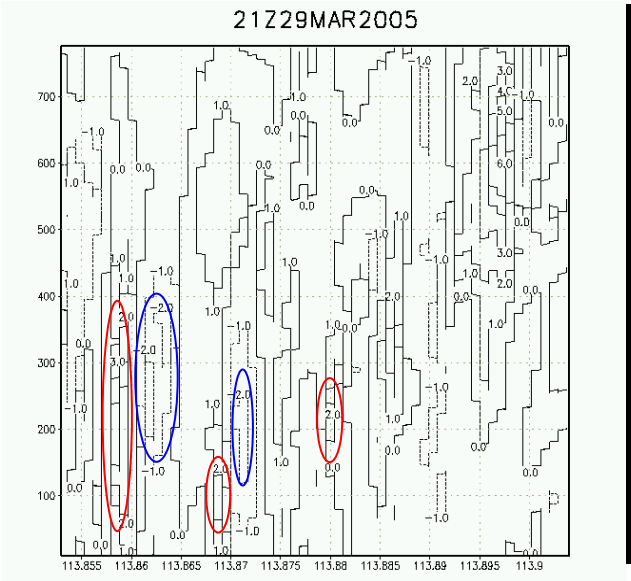

Figure 5 Vertical velocity distribution in the model simulation along the dotted line in Figure 4. The larger vertical velocity regions at the lower part of the boundary layer are enclosed in red (+ve) and blue (-ve) ellipses.

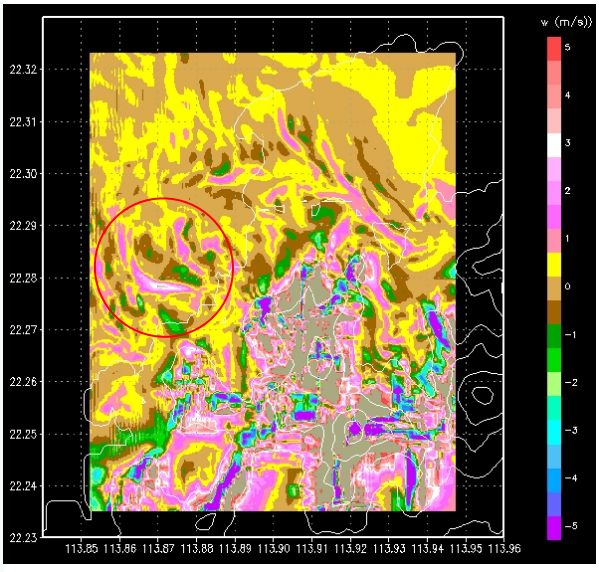

Figure 6 Vertical velocity field from the model simulation at 50 m AMSL (+ve means upwards). The bands of vertical motion with northwest-to-southeast orientation are enclosed in red.

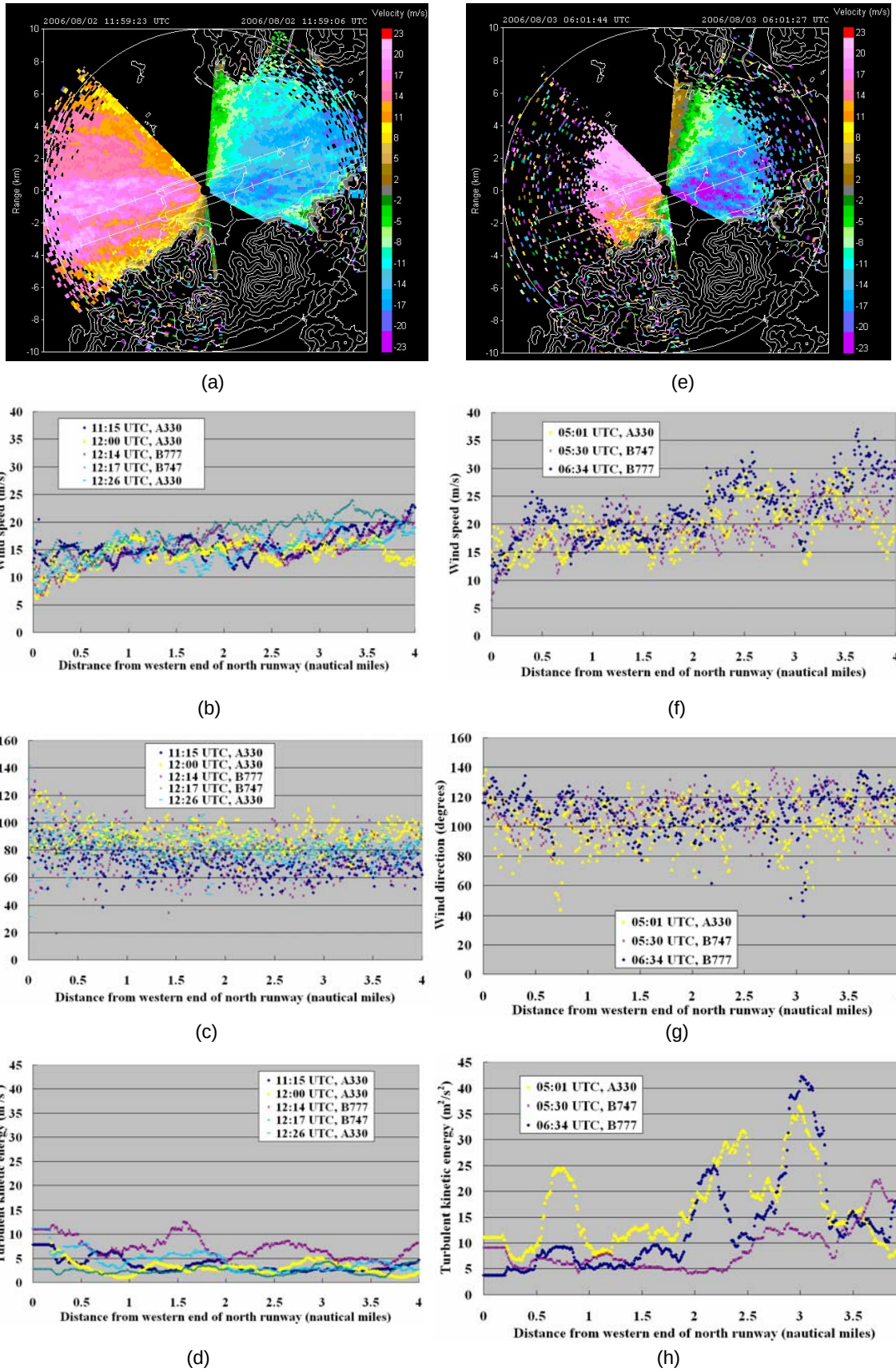

Figure 7 LIDAR radial velocity image from 1-degree conical scans at about (a) 12 UTC, 2 August 2006 and (e) 06 UTC, 3 August 2006. (b) – (d) and (f) – (h) are the flight data at the corresponding times, with the plots of wind speed, wind direction and TKE up to 4 nautical miles from the western end of the north runway of HKIA.

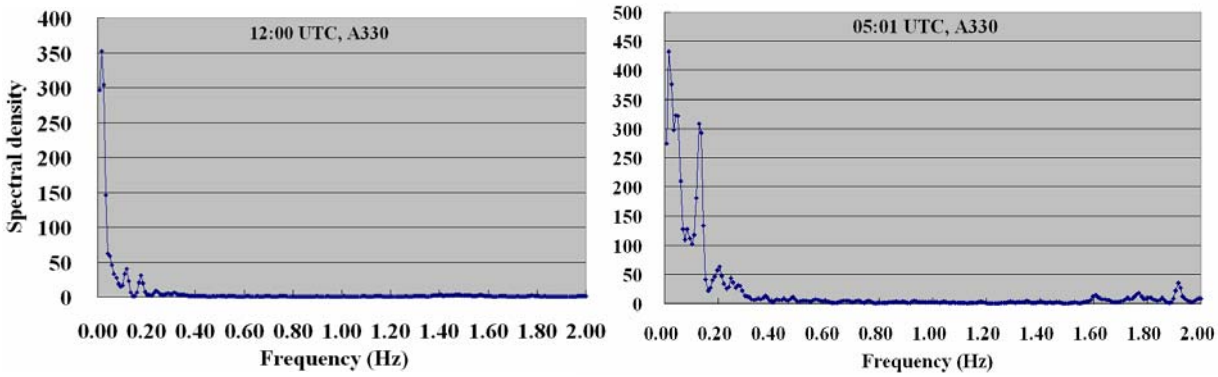

(a) (b)

Figure 8 A typical power spectrum of the horizontal wind speed at around (a) 12 UTC, 2 August 2006 and (b) 06 UTC, 3 August 2006.

Flight	Length scale	Spectral density
11:15 UTC, A330	*7403.91 m*	*289.92*
	1233.98 m	*72.29*
	740.39 m	54.66
12:00 UTC, A330	*3688.26 m*	*352.31*
	526.89 m	40.08
	351.26 m	30.74
12:14 UTC, B777	*7392.24 m*	*239.36*
	1478.45 m	*98.25*
	492.82 m	22.64
12:17 UTC, B747	*1483.13 m*	*132.36*
	617.97 m	13.42
	337.07 m	20.02
12:26 UTC, A330	*3690.86 m*	*316.01*
	922.72 m	*144.84*
	434.22 m	33.02

(a)

Flight	Length scale	Spectral density
05:01 UTC, A330	*3699.62 m*	*431.68*
	493.28 m	*308.59*
	308.30 m	63.38
05:30 UTC, B747	*3699.83 m*	*175.47*
	1233.28 m	*160.00*
	672.70 m	40.04
06:34 UTC, B777	*2469.97 m*	*736.46*
	673.63 m	108.54
	390.00 m	63.95

(b)

Table 1 The three main peaks in the spectral analysis results of the wind speed fluctuations at about (a) 12 UTC, 2 August 2006 and (b) 06 UTC, 3 August 2006. The major peaks used in the discussion of length scale (i.e. with larger spectral density values) are shown in italic.

Flight	Length scale	Spectral density
11:15 UTC, A330	*7403.91 m*	*22.50*
	1233.98 m	*23.45*
	616.99 m	*32.98*
12:00 UTC, A330	*1851.94 m*	*14.25*
	740.78 m	*19.62*
	284.91 m	*14.42*
12:14 UTC, B777	*3696.12 m*	*41.39*
	1056.03 m	*17.66*
	336.01 m	*17.39*
12:17 UTC, B747	*741.56 m*	*39.55*
	494.38 m	*41.08*
	322.42 m	*63.92*
12:26 UTC, A330	*1482.50 m*	*39.13*
	436.03 m	*48.68*

(a)

Flight	Length scale	Spectral density
05:01 UTC, A330	*3762.86 m*	*149.53*
	940.71 m	*159.90*
	358.37 m	*91.55*
05:30 UTC, B747	*4654.62 m*	*190.76*
	620.62 m	*141.26*
	423.15 m	*130.02*
06:34 UTC, B777	*5790.94 m*	*158.06*
	723.87 m	*248.77*

(b)

Table 2 Similar to Table 1, but for vertical velocity fluctuations.